arXiv:nucl-th/0206043v2 13 Aug 2002

# Medium effects to $N(1535)$ resonance and $\eta$ mesic nuclei

D. Jido,[1,*] H. Nagahiro,[2] and S. Hirenzaki[1,2]

[1] *Departamento de Física Teórica and IFIC, Centro Mixto Universidad de Valencia-CSIC, Ap. Correos 22085, E-46071 Valencia, Spain*

[2] *Department of Physics, Nara Women's University, Nara 630-8506, Japan*

(Dated: February 8, 2008)

The structure of $\eta$-nucleus bound systems ($\eta$ mesic nuclei) is investigated as one of the tools to study in-medium properties of the $N(1535)$ ($N^*$) resonance by using the chiral doublet model to incorporate the medium effects of the $N^*$ resonance in a chiral symmetric way. We find that the shape and the depth of the $\eta$-nucleus optical potential are strongly affected by the in-medium properties of the $N^*$ and the nucleon. Especially, as a general feature of the potential, the existence of a repulsive core of the $\eta$-nucleus potential at the nuclear center with an attractive part at the nuclear surface is concluded. We calculate the level structure of bound states in this 'central-repulsive and surface-attractive' optical potential and find that the level structure is sensitive to the in-medium properties of the $N^*$. The (d,$^3$He) spectra are also evaluated for the formation of these bound states to investigate the experimental feasibility. We also make comments on the possible existence of halo-like $\eta$ states in $\beta$-unstable halo nuclei.

PACS numbers: 12.39.Fe,14.20.Gk,14.40.Aq,25.10.+s,36.10.Gv
Keywords: $\eta$ mesic nucleus, $N(1535)$, chiral symmetry, medium effect

## I. INTRODUCTION

The study of the in-medium properties of hadrons has attracted continuous attention and is one of the most interesting topics of nuclear physics. So far, several kinds of hadron-nucleus bound systems have been investigated such as pionic atoms, kaonic atoms, and $\bar{p}$ atoms [1]. The structure of these systems is described by means of a complex optical potential, which reproduces well the experimental data obtained by the X-ray spectroscopic methods [2]. The search of the deeply bound pionic atoms has been performed from the end of 80's [3–6], and the use of the recoilless (d,$^3$He) reaction [7] led to the successful discovery of the deeply bound states, which enable us to deduce in-medium pion properties [8–10]. Now extensions of the method to other meson-nucleus bound states are being widely considered both theoretically and experimentally [11–14].

In this paper we consider the $\eta$ mesic nucleus as one of the doorways to investigate the in-medium properties of the $N(1535)$ ($N^*$). The special features of the $\eta$ mesic nucleus are the following; (1) the $\eta$-$N$ system dominantly couples to $N(1535)$ at the threshold region [15]. (2) The isoscalar particle $\eta$ filters out contaminations of the isospin 3/2 excitations in the nuclear medium. (3) Due to the $s$-wave nature of the $\eta N N^*$ coupling there is no threshold suppression like the $p$-wave coupling. The strong coupling of the $N^*$ to $\eta N$ makes the use of this channel particularly suited to investigate this resonance in a cleaner way than the use of $\pi N$ for the study of other resonances like the $N(1440)$ and $N(1520)$.

On the other hand, the in-medium properties of hadron are believed to be related to partial restoration of chiral symmetry in the contemporary point of view (see, e.g.[16]), in which a reduction of the order parameter of the chiral phase transition in hot and/or dense matter takes place and causes modifications of the hadron properties. The $N^*$, which is the lowest lying parity partner of the nucleon, has been investigated from the point of view of chiral symmetry [17, 18], where the $N$ and $N^*$ form a multiplet of the chiral group. In refs.[19, 20] a reduction of the mass difference of the $N$ and $N^*$ in the nuclear medium is found in the chiral doublet model, while a reduction of the $N^*$ mass is also found as the quark condensate decreases in the QCD sum rule [21]. Considering the fact that the $N^*$ mass in free space lies only fifty MeV above the $\eta N$ threshold, the medium modification of the $N^*$ mass will strongly affect the in-medium potential of the $\eta$ meson through the strong $\eta N N^*$ coupling described above.

As one of the standard theoretical tools to obtain the structure of the bound states, we solve the Klein-Gordon equation with the meson-nucleus interaction, which is expressed in terms of an optical potential and is evaluated using the chiral doublet model developed in refs.[17, 18], which embodies the reduction of the $N^*$ mass associated with the partial restoration of chiral symmetry, assuming the $N^*$ dominance for the $\eta N$ coupling described above. The calculation is done in nuclear matter with the mean-field approximation, and the local density approximation is used to apply it to the finite nuclei. For the observation of the these bound states, we also consider the missing mass spectroscopy by the (d,$^3$He) reaction which was proven to be a powerful tool experimentally. To evaluate the expected spectra theoretically, we adopt the Green function method for the unstable bound states [22].

*Electronic address: jido@rcnp.osaka-u.ac.jp; present address: Research Center for Nuclear Physics (RCNP), Ibaraki, Osaka 567-0047, Japan

In section 2 we describe the $\eta$-nucleus optical potential which is obtained in our framework with the chiral doublet model and the $N^*$ dominance. In section 3 we show the numerical results for the $\eta$ meson bound states in the nucleus and the (d,$^3$He) spectra. Section 4 is devoted to the summary and conclusion.

## II. OPTICAL POTENTIAL OF $\eta$ WITH $N^*$ DOMINANCE

The $\eta$-mesic nuclei were studied by Haider and Liu [23] and by Chiang, Oset and Liu [24] systematically. There, the $\eta$-nucleus optical potential was expected to be attractive from the data of the $\eta$-nucleon scattering length and the existence of the bound states was predicted theoretically. As the formation reaction, the use of the $(\pi^+, p)$ reaction was proposed and the attempt to find the bound states in the reaction led to a negative result [25]. The $(\pi^+, p)$ experiment [25] was designed to be sensitive to the expected narrow states, but was probably not sensitive enough to see much broader structures.

Before presenting the detail of our model calculation, let us show the possibility to have a repulsive $\eta$ optical potential in the nucleus due to the significant reduction of the mass difference of $N$ and $N^*$. Considering the self-energy of the $\eta$ meson at rest in nuclear matter in the $N^*$ dominance model, in analogy with the $\Delta$-hole model for the $\pi$-nucleus system, we obtain the $\eta$ optical potential in the nuclear medium in the heavy baryon limit [24] as;

$$V_\eta(\omega) = \frac{g_\eta^2}{2\mu}\frac{\rho(r)}{\omega + m_N^*(\rho) - m_{N^*}^*(\rho) + i\Gamma_{N^*}(s;\rho)/2} \ , \quad (1)$$

where $\omega$ denotes the $\eta$ energy, and $\mu$ is the reduced mass of the $\eta$ and the nucleus and is very close to the $\eta$ mass, $m_\eta$, for heavy nuclei. $\rho(r)$ is the density distribution for nucleons in the finite nucleus, for which we assume here a Fermi distribution. The "effective mass" of $N$ and $N^*$ in medium, denoted as $m_N^*$, $m_{N^*}^*$, are defined through their propagators so that $\mathrm{Re}\, G^{-1}(p^0 = m^*, \vec{p} = 0) = 0$. The in-medium $N^*$ width $\Gamma_{N^*}$ includes the many-body decay channels. The $\eta N N^*$ vertex $g_\eta$ is given by

$$\mathcal{L}_{\eta N N^*}(x) = g_\eta \bar{N}(x)\eta(x)N^*(x) + \mathrm{h.c.}, \quad (2)$$

where $g_\eta \simeq 2.0$ to reproduce the partial width $\Gamma_{N^* \to \eta N} \simeq 75$ MeV [26] at tree level.

Supposing no medium modifications for the masses of $N$ and $N^*$ as well as small binding energy for the $\eta$, *i.e.* $\omega \simeq m_\eta$, we obtain an attractive potential independent of density since we always have $\omega + m_N - m_{N^*} < 0$ in the nucleus. The shape of this potential is essentially the same as the Woods-Saxon type potential for a finite nucleus assuming the local density approximation. On the other hand, if a sufficient reduction of the mass difference of $N$ and $N^*$ stems from the medium effects, there exists a critical density $\rho_c$ where $\omega + m_N^* - m_{N^*}^* = 0$, and then at densities above $\rho_c$ the $\eta$ optical potential turns to be repulsive. If $\rho_c$ is lower than the nuclear saturation density $\rho_0$, the optical potential for the $\eta$ is attractive around the surface of the nucleus and repulsive in the interior. Therefore the bound states of the $\eta$ in nuclei, if they exist, will be localized at the surface and the level structure of the $\eta$ bound states will be quite different from that in the case of the Woods-Saxon type potential.

To make the argument more quantitative, we estimate the in-medium $N$ and $N^*$ masses and the $N^*$ width in the chiral doublet model [17, 18] (see also [27]), which embodies the reduction of the mass difference of $N$ and $N^*$ associated with the partial restoration of chiral symmetry. The chiral doublet model is an extension of the $SU(2)$ linear sigma model for the nucleon incorporating the $N^*$. In the model $N$ and $N^*$ are expressed as superpositions of $N_1$ and $N_2$ which are eigenvectors under the chiral transformation. There are two types of the linear sigma model choosing either the assignment of the same sign of the axial charge to $N_1$ and $N_2$ or the opposite sign to each other. The model with the later construction was first investigated by DeTar and Kunihiro [17], and was named the "mirror assignment" later on to distinguish it from the first assignment ("naive assignment") [18]. Here we shall discuss only the chiral doublet model with the mirror assignment. We have already checked that the naive assignment produces a qualitatively similar optical potential of the $\eta$ to that with the mirror assignment. The quantitative studies with the naive assignment will be discussed elsewhere.

The Lagrangian of the chiral doublet model with the mirror assignment is given by

$$\begin{aligned}\mathcal{L} \ = \ & \sum_{j=1,2}\left[\bar{N}_j i\partial\!\!\!/ N_j - g_j \bar{N}_j(\sigma + (-)^{j-1} i\gamma_5 \vec{\tau}\cdot\vec{\pi})N_j\right] \\ & -m_0(\bar{N}_1\gamma_5 N_2 - \bar{N}_2\gamma_5 N_1) \ , \end{aligned} \quad (3)$$

where $N_1$ and $N_2$ are eigenvectors under the $SU(2)$ chiral transformation and have opposite axial charge to each other. The physical $N$ and $N^*$ are expressed as a superposition of $N_1$ and $N_2$ as $N = \cos\theta N_1 + \gamma_5 \sin\theta N_2$ and $N^* = -\gamma_5 \sin\theta N_1 + \cos\theta N_2$ where $\tan 2\theta = 2(g_1 + g_2)m_0/\langle\sigma\rangle$. In this basis, the $N$ and $N^*$ masses and the $\pi N N^*$ vertex are given as functions of the sigma condensate as in the standard liner sigma model:

$$\begin{aligned} m_{N,N^*}^* \ &= \ \frac{1}{2}\left(\sqrt{(g_1+g_2)^2\langle\sigma\rangle^2 + 4m_0^2} \mp (g_2 - g_1)\langle\sigma\rangle\right) \quad (4) \\ g_{\pi N N^*}^* \ &= \ (g_2 - g_1)/\sqrt{4 + ((g_1+g_2)\langle\sigma\rangle/m_0)^2} \ , \quad (5) \end{aligned}$$

where $\langle\sigma\rangle$ is the sigma condensate in nuclear matter. It is worth noting that the mass splitting between $N$ and $N^*$ is generated by the spontaneous breakdown of chiral symmetry with a linear form of the sigma condensate. The parameters in the Lagrangian have been chosen so that the observables in vacuum, $m_N = 940$ MeV, $m_{N^*} = 1535$ MeV and $\Gamma_{N^* \to \pi N} \simeq 75$ MeV are reproduced with $\langle\sigma\rangle_0 = f_\pi = 93$ MeV, and they are $g_1 = 9.8$, $g_2 = 16.2$, $m_0 = 270$ MeV[18].

In the linear $\sigma$ model, the nuclear medium effects come from the nucleon loops which modify the self-energies of $N$ and $N^*$ and the vertex of $\pi NN^*$ [28]. In the mean-field approximation, such contributions can be introduced by making the replacement of the vacuum condensate of the sigma meson to the in-medium condensate which depends on the density $\rho$ as

$$\langle\sigma\rangle = \Phi(\rho)\langle\sigma\rangle_0 \ , \tag{6}$$

where $\Phi(\rho)$ should be determined elsewhere. Here we take a linear parameterization as $\Phi(\rho) = 1 - C\rho/\rho_0$ with $C$=0.1-0.3 [28]. The $C$ parameter represents the strength of the chiral restoration at the nuclear saturation density $\rho_0$. Finally, with this replacement, the density dependence of the in-medium mass difference of $N$ and $N^*$ is obtained as

$$m^*_N(\rho) - m^*_{N^*}(\rho) = (1 - C\rho/\rho_0)(m_N - m_{N^*}) \ . \tag{7}$$

This implies that for $C > 0.08$ the real part of the in-medium $\eta$ self-energy with $\omega = m_\eta$ in eq.(1) changes its sign at smaller densities than the saturation density $\rho_0$.

Now let us consider the $N^*$ width in the medium. In free space there are three strong decay modes of $N^*$, $\pi N$, $\eta N$ and $\pi\pi N$ [26]. The first two are dominant modes and give almost the same decay rate. Here the medium effects on the decay widths of these modes are taken into account by considering the Pauli blocking effect on the decaying nucleon, and by changing the $N$ and $N^*$ masses and the $\pi NN^*$ coupling in medium through eqs. (4) and (5), according to the chiral doublet model as discussed above.

The partial decay widths of $N^*$ to certain decay channels can be obtained by evaluating the self-energy of $N^*$ associated with the decay channel and by taking its imaginary part as $\Gamma_{N^*} = -2\mathrm{Im}\Sigma_{N^*}$. The partial decay width for $N^* \to \pi N$ is calculated as

$$\Gamma_\pi(s) = 3\frac{g^{*2}_{\pi NN^*}}{4\pi}\frac{E_N + m^*_N}{\sqrt{s}}q \ , \tag{8}$$

where $E_N$ and $q$ are the energy and the momentum of the final nucleon on the mass shell in the $N^*$ rest frame, respectively. The momentum $q$ is given by $q = \lambda^{1/2}(s, m^{*2}_N, m^2_\pi)/2\sqrt{s}$ with the Källen function $\lambda(x, y, z)$. The Pauli blocking effect for $N^* \to \pi N$ mode is negligible due to the large decaying momentum $q \simeq 460$ MeV in vacuum. The decay mode $N^* \to \eta N$, however, does not contribute in the medium because of no available phase space due to the Pauli blocking [24].

The decay branching rate of the $N^* \to \pi\pi N$ channel is known to be only $1 \sim 10$ percent in vacuum [26]. Here in the present calculation, we do not include this decay mode since its contribution is estimated to be only a few percent of the total decay rate in our model. In spite of no direct $\pi\pi NN^*$ vertex in our model, this channel can be evaluated by considering the process $N^* \to \sigma N \to \pi\pi N$ using the linear sigma model for $\sigma$ and $\pi$.

Other medium effects on the decay of $N^*$ are the many-body decays, such as $N^*N \to NN$ and $N^*N \to \pi NN$. The $N^*$ many-body absorption, involving two-nucleon $\eta$ absorption mechanisms, is evaluated by inserting particle-hole excitations to the $\pi$ ($\eta$) propagator in the $\pi N$ ($\eta N$) self-energy of $N^*$. The width from $NN^* \to NN$ channel was already calculated in ref.[24] and was found several MeV at $\rho = \rho_0$. Here we neglect the contribution of this channel. The other $N^*$ absorption, $NN^* \to \pi NN$, is comparably larger than $NN^* \to NN$ because of its phase space [24]. We estimated the $NN^* \to \pi NN$ process within our model following the formulation of ref.[24]:

$$\Gamma_{N^*N\to\pi NN}(\sqrt{s}) = \tag{9}$$
$$3\beta^2\left(\frac{g_{\pi NN}}{2m^*_N}\right)^2\rho\int dp_1 p_1^3\int\frac{dp_2}{(2\pi)^3}p_2\frac{m^*_N}{\omega_2}$$
$$\times\frac{-\vec{p}_1^{\,2} + 2m^*_N(\sqrt{s} - \omega_2 - m^*_N)}{\left[\left(\frac{p_1^2}{2m^*_N}\right)^2 - p_1^2 - m^2_\pi\right]^2}\Phi(p_1, p_2) \ , \tag{10}$$

where $p_1$ ($\omega_1$) and $p_2$ ($\omega_2$) are pion momenta (energies), $\Phi$ is the phase space variable defined in [24] and

$$\beta = \frac{g_1 m_0}{\langle\sigma\rangle m^*_N(m^*_{N^*} + m^*_N)}\chi \tag{11}$$

with the effective coupling of $\pi\pi N$ through $\sigma$ meson in this model, which is $\chi \sim 1.29$. This contribution is estimated to be typically fifteen MeV at the saturation density, although it depends on the $\eta$ energy and $C$ parameter. We include this channel in the present calculation.

## III. NUMERICAL RESULTS

In the previous section, we discuss the $\eta$ optical potential in nuclear matter using the $N^*$ dominance model and the chiral doublet model. The final expression of the $\eta$ optical potential in the nuclear medium is obtained by substituting the mass gap between $N$ and $N^*$ obtained in eq.(7) and the in-medium $N^*$ width described in eqs.(8) and (10) to eq.(1). In this section, we show some numerical results for the $\eta$ meson in the nucleus from the optical potential derived above.

### A. Optical potential of the $\eta$ in the nucleus

For finite nuclei we assume the local density approximation and the Fermi distribution of nucleons in the nucleus with the radial parameter $R = 1.18A^{1/3} - 0.48$ [fm] and the diffuseness parameter $a = 0.5$ [fm]. In Fig.1, we show the $\eta$-nucleus potential for the $^{132}$Xe case, as an example. In other nuclei, the potential shape is essentially the same as the plotted one, but the radius of the repulsive core depends on the mass number $A$. As can be seen in the figure, for the $C \neq 0$ cases the real potential

turns out to be repulsive at the inner part of the nucleus, associated with the reduction of the mass difference of $N$ and $N^*$ in the nucleus and an attractive "pocket" appears on the surface. This pocket-shape potential is new and so interesting that the existence of the repulsive core is consistent with the experiment [29], where the production of the $\eta$ meson on various nuclei is surface dominated due to the strong final state interaction.

Another interesting feature of the potential is its strong energy dependence. By changing the energy of the $\eta$ from $\omega = m_\eta$ to $m_\eta - 50$ [MeV], we find again the familiar attractive potential shape even with $C = 0.1$ as shown in the figure. We also find that the imaginary part of the potential has a strong dependence both on the $C$ parameter and the $\eta$ energy.

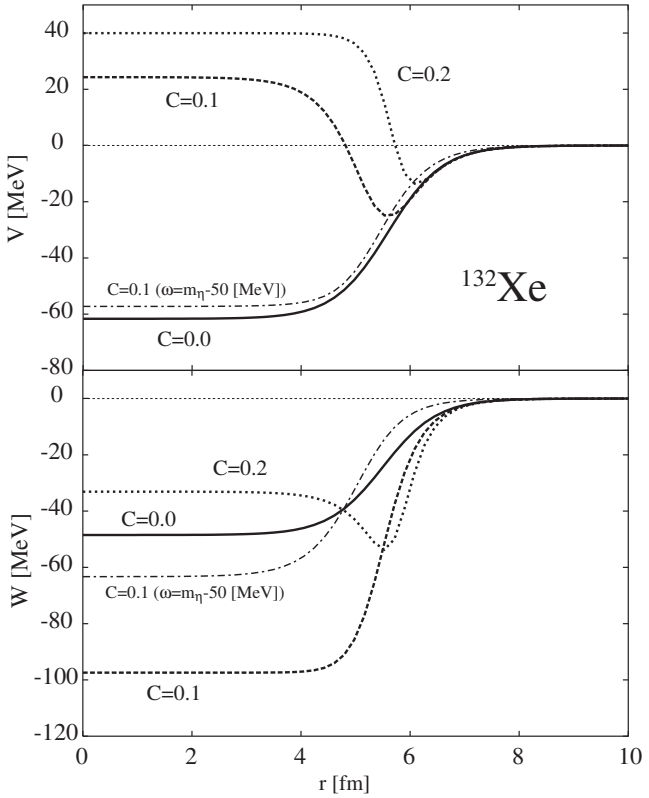


FIG. 1: The $\eta$-nucleus optical potential for $^{132}$Xe system as a function of the radius coordinate $r$. The upper and lower panels show the real part and imaginary part, respectively, for $C = 0.0$ (solid line), 0.1 (dashed line) and 0.2 (dotted line) with setting $\omega = m_\eta$. The dot-dashed line indicates the potential strength for $C = 0.1$ with $\omega = m_\eta - 50$ [MeV].

### B. Bound states of $\eta$ in nuclei

In order to calculate the eigenenergies and wavefunctions of the $\eta$ bound states, we solve numerically the Klein-Gordon equation with the $\eta$-nucleus optical potential obtained here, and make an iteration to obtain the self-consistent energy eigenvalues for the strongly energy dependent optical potential. We follow the method of Kwon and Tabakin to solve it in momentum space [30]. We increase the number of the mesh points in the momentum space which is here about 10 times larger than ref.[30]. The number of mesh points was limited ($\sim 40$ points) and the parameters for the mesh points distribution were adjusted for the shallow mesic atoms [30]. We check the stability of the obtained results carefully.

We show the calculated binding energies and level widths in Table I for 1s and 2p states in several nuclei over the periodic table. For the $C = 0$ case, in which no medium modifications are included in the $N$ and $N^*$ properties, since the potential is proportional to the nuclear density distribution as we have seen in Fig.1, the level structure of the bound states is similar to that obtained in ref.[12]. For $C \geq 0.1$ cases, the formation of $\eta$ bound states is quite difficult because of both the repulsive nature of the potential inside the nucleus and the huge imaginary part of the potential.

In order to see the $C$ parameter dependence of the bound states in $C < 0.1$, we consider $^{132}$Xe as an example and calculate the bound states for $C = 0.02$, 0.05 and 0.08 cases. The results are also compiled in the Table I. We should mention here that, due to the small attraction, in the pocket like case we do not find bound states. They, however, are obtained in the case of the Woods-Saxon type.

| C | A | L=0 | | L=1 | |
|---|---|---|---|---|---|
| | | B.E.[MeV] | width[MeV] | B.E.[MeV] | width[MeV] |
| 0.0 | 6 | 3.7 | 35.1 | - | - |
| | 11 | 13.7 | 41.5 | - | - |
| | 15 | 18.5 | 42.7 | - | - |
| | 19 | 21.9 | 43.1 | - | - |
| | 31 | 27.9 | 42.8 | 10.1 | 52.2 |
| | 39 | 30.3 | 42.5 | 14.6 | 50.7 |
| | 64 | 34.4 | 41.3 | 22.4 | 47.7 |
| | 88 | 36.4 | 40.5 | 26.4 | 45.8 |
| | 132 | 38.4 | 39.6 | 30.5 | 43.8 |
| | 207 | 39.9 | 38.5 | 33.9 | 41.8 |
| 0.02 | 132 | 41.2 | 49.0 | 33.0 | 55.0 |
| 0.05 | 132 | 45.1 | 69.3 | 35.5 | 81.5 |
| 0.08 | 132 | 46.1 | 106.3 | - | - |
| 0.1 | 132 | - | - | - | - |

TABLE I: The $\eta$-nucleus binding energies and widths for various nuclei for $C = 0$. Results for the $C \neq 0$ cases are also shown for the $\eta$-$^{132}$Xe system.

### C. Spectra of (d,$^3$He) for the $\eta$ mesic nuclei formation

Although the formation of the bound states of the $\eta$ in nuclei is difficult with $C \sim 0.2$, which is the expected

strength of the chiral restoration in the nucleus, it would be interesting to see if the repulsive nature of the optical potential can be observed in experiment. Here we consider the recoilless (d,$^3$He) reaction, in which a proton is picked up from the target nucleus and the $\eta$ meson is left with a small momentum.

The recoilless (d,$^3$He) reaction is expected to be one of the most powerful experimental tools for formation of the $\eta$-mesic nucleus [7]. The spectra of this reaction are investigated in detail in ref.[12]. There they estimate the experimental elementary cross section of $d + p \rightarrow {}^3\mathrm{He}+\eta$ reaction to be 150 (nb/sr) in this kinematics based on the data taken at SATURNE [31], and use the Green function method [22], in which the $\eta$-meson Green function provides information of the structure of unstable bound states. Applying the same approach, we evaluate the expected spectra of the (d,$^3$He) reaction by assuming our optical potential for the $\eta$ in the nucleus. Here we calculate the spectra of the $^{12}$C(d,$^3$He) reaction for the $\eta$ production in the final state. The $^{12}$C is shown to be a suitable target to populate the $[(p_{3/2})_p^{-1} \otimes p_\eta]$ configuration largely [12]. We assume the single particle nature for the protons in the target $^{12}$C and consider $0s_{1/2}$ and $0p_{3/2}$ states. And we take into account sufficient number of partial waves $l_\eta$ of $\eta$. We find that only $l_\eta \leq 3$ partial waves are relevant in this energy region and we check numerically that contributions from higher partial waves are negligible.

The obtained spectra are shown in Fig.2 as functions of the excited energy which are defined as,

$$E_{\mathrm{ex}} = m_\eta - B_\eta + (S_p(j_p) - S_p(p_{3/2})) \ , \qquad (12)$$

where $B_\eta$ is the $\eta$ binding energy and $S_p$ the proton separation energy. The $\eta$ production threshold energy $E_0$ is indicated in the figure by the vertical line. The calculated spectra are shown in Fig.2 for three different sets of the parameter $C$ in the optical potential and the diffuseness parameter $a$ of the nuclear density distribution. In Fig.2(a), we show the result with $C = 0.0$ and $a = 0.5$ [fm] which corresponds to the spectrum with the potential which does not include any medium modifications of $N$ and $N^*$. The results with the medium corrections are shown in Fig.2(b) for the $C = 0.2$ case, where the $\eta$ optical potential has the repulsive core in the center of nucleus. It is seen in the Fig.2(a) and (b) that, due to the repulsive nature of the $\eta$ potential with $C = 0.2$, the whole spectrum is shifted to the higher energy region and the $s$-wave $\eta$ contribution around $E_{\mathrm{ex}} - E_0 \sim 0$ [MeV] is suppressed in Fig.2(b), which corresponds to the disappearance of the $\eta$-bound state for $C = 0.2$. The difference of these spectra is expected to be observed in the high resolution experiments.

We also calculate the spectrum for the $C = 0.2$ case with the diffuseness $a = 1.0$ [fm], to simulate the halo-like structure of unstable nuclei. In this case, the $\eta$-nucleus optical potential has a wider attractive region than that with $a = 0.5$ [fm] because of the existence of the longer tail at low nuclear densities. The results are shown in Fig.2(c), where we can see that the whole spectrum is shifted to smaller energy regions compared to Fig.2(b) indicating the attractive nature of the potential.

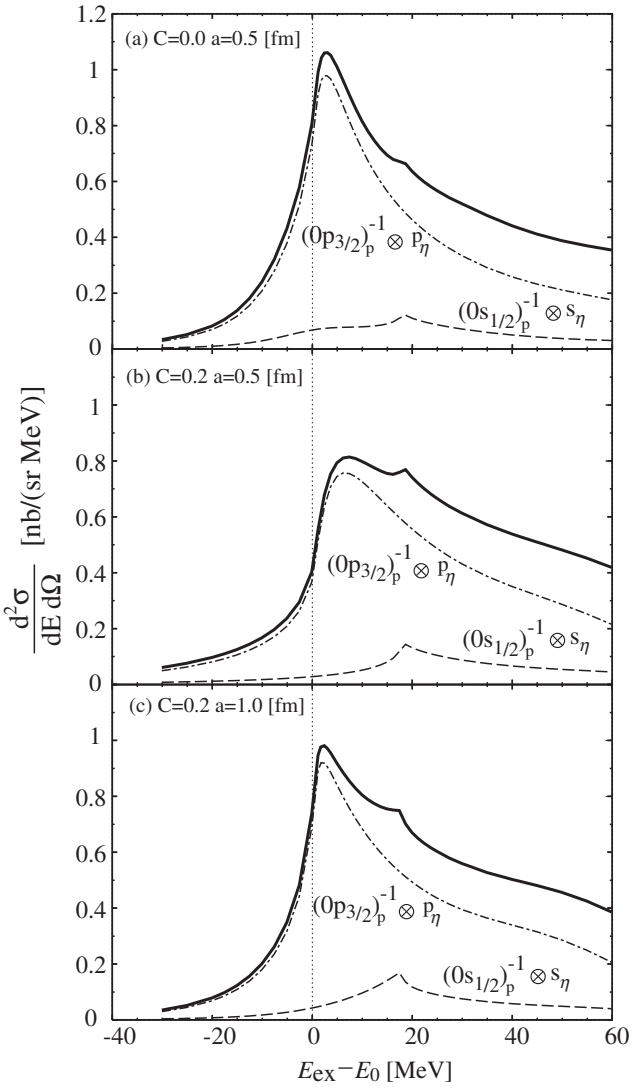


FIG. 2: The calculated excitation energy spectrum of the $\eta$ production in the $^{12}$C(d,$^3$He) reaction at $T_d = 3.5$ [GeV] for three different sets of the parameter $C$ in the $\eta$-nucleus optical potential and the diffuseness parameter $a$ of the nuclear density; (a) $C = 0.0$ and $a = 0.5$ [fm], (b) $C = 0.2$ and $a = 0.5$ [fm], (c) $C = 0.2$ and $a = 1.0$ [fm]. The vertical line indicates the $\eta$ production threshold energy. In each figure, the contribution from the $(0p_{3/2})_p^{-1} \otimes p_\eta$ is shown in a dash-dotted curve, the $(0s_{1/2})_p^{-1} \otimes s_\eta$ contribution is shown in the dashed curve, and the solid curve is the sum of $\eta$-partial waves. The continuum background contributions are estimated to be about 3.4 [nb/(sr MeV)] for the $^{12}$C target [12].

### D. Discussion

Here we make some remarks on the "pocket-like" potential. First of all, we would like to consider the interesting possibility to have $\eta$ bound states in $\beta$-unstable nuclei with a halo structure [32]. So far, we have considered stable nuclei with the small diffuseness parameters ($a = 0.5$ [fm]), in which the density suddenly changes at the surface. As we have seen in Fig.1, the optical potential with a finite $C$ value is attractive only in the low density region at the nuclear surface. Thus, halo nuclei have a larger attractive region than the stable nuclei and we expect to find more $\eta$ bound states, which will be like coexistence states of the halo-like $\eta$ mesic bound states with halo nucleons. We simulate the behavior of the $\eta$ bound states for nuclei with halo structure by changing the diffuseness parameters artificially for $^{132}$Xe case. However, in spite of our systematic search of the $\eta$ bound states for diffuseness parameters, $a = 1.0$ and 1.5 [fm], no bound states in the pocket-like potential are found for the $C = 0.1, 0.15$ and 0.2 cases.

Second, we have another quite interesting feature of the $\eta$-nucleus bound states because of its strong energy dependence. In the iterative calculation to get the self-consistent eigenenergies for the energy dependent potential, we have possibilities to find several solutions for certain set of the quantum numbers $(n, l)$. Actually, we have found the three 1s-like states for the $\eta$-$^{88}$Y system for the $C = 0.1$ case by omitting the imaginary part of the optical potential. The wavefunctions of all three states do not have any node and they are shown to be; (1) The bound 1s state with B.E. = 40.4 [MeV] in the Woods-Saxon type potential, (2) The bound 1s state with B.E. = 22.2 [MeV] in the attractive potential which is deeper at the surface than in the nuclear center, (3) The bound 1s state with B.E. = 6.0 [MeV] in the surface-attractive and central-repulsive potential.

Third, we would like to make a general comment on the level structure of the bound states in the pocket-like potential. To make the argument clear, we consider only the real part of the pocket-like potential. Let us consider the radial part of the Schrödinger equation with an attractive pocket potential at a certain radius $R$ and a width $a$. As we can see in any text book of quantum mechanics, this equation is exactly the same as the one dimensional Schrödinger equation with the same potential pocket except for the centrifugal potential and the boundary condition for the wavefunction at the origin $r = 0$. Since the one dimensional Schrödinger equation has translational invariance with this potential, the eigenenergies do not depend on the position of the attractive pocket. This is also the case for the radial equation for heavy nuclei in which the attractive potential exists far from the nuclear center, where the wavefunction boundary condition is automatically satisfied and do not affect the eigenenergies. Thus, the level structure would be expected to resemble each other for all heavy nuclei, which is quite different from the case of the Woods-Saxon type potential, where the binding energies become larger in heavier nuclei.

Another interesting feature of the level structure is that, since the pocket potential in heavy nuclei is far from the center of the system and then the centrifugal repulsive potential could be weak at the position of the pocket, then the different angular momentum states would approximately degenerate in heavy nuclei. All these features of the level structure are very interesting and really characteristic for the 'surface-attractive' $\eta$-nucleus optical potential.

Very recently an investigation of the $\eta$ meson properties in the nuclear medium within a chiral unitary approach has been reported [33]. There, they also found a strong energy dependent optical potential of the $\eta$. It would be interesting to compare their consequences with ours since their theoretical framework is quite different from our model and there the $N^*$ is introduced as a resonance generated dynamically from meson-baryon scatterings.

## IV. SUMMARY

We investigate the consequences of the medium effects to $N(1535)$ ($N^*$) through the eta-mesic nuclei assuming the $N^*$ dominance in the $\eta$-$N$ system. The chiral doublet model is used to estimate the medium modification of the $N$ and $N^*$ properties. This model embodies chiral symmetry and its spontaneous breaking within the baryonic level ($N$ and $N^*$) and shows the reduction of the mass difference of $N$ and $N^*$ with the partial restoration of chiral symmetry.

We find that sufficient reduction of the mass difference due to chiral restoration makes the $\eta$ optical potential in nuclei repulsive at certain densities, while in the low density approximation the optical potential is estimated to be attractive. This leads us the possibility of a new type of potential of the $\eta$ in nucleus that is attractive at the surface and has a repulsive core at the center of the nucleus. We discuss general features of this "pocket" potential that the level structure is quite different from that with the potential simply obtained from the $V \sim t\rho$ approximation with $t$ the scattering amplitude of the $\eta$-$N$ system.

We calculate the in-medium optical potential of the $\eta$ meson with a mean-field approximation and use the local density approximation to apply it to finite nuclei. We also find that the potential obtained here has a strong energy dependence, which leads us to the self-consistent formulation in the calculation of the $\eta$ bound states in the nucleus. Unfortunately it is hard to form $\eta$ bound states in the nuclei with the expected strength of the chiral restoration in nucleus ($C \sim 0.2$), due to the repulsive nature of the potential inside the nucleus and its large imaginary potential. We find that there is no bound state for the case of $C \geq 0.1$ even in the halo-like nuclei, which are expected to have moderate density distributions and to have a wider attractive potential pocket at the surface.

We evaluate the spectra of the recoilless (d,$^3$He) reaction with a $^{12}$C target using our optical potential for the $C = 0.0$ and 0.2 cases. The shapes of these spectra are apparently different and the repulsive nature in the $C = 0.2$ case is seen. The results with the large diffuseness parameter for the nuclear density distribution also show the sensitivity of the spectrum to the existence of the halo structure. We find that the existence of the halo also changes the spectrum shape, and thus a comprehensive study of $\eta$ bound states in unstable nuclei also would be interesting to investigate the medium effects of the $N^*$. We believe that the present results are very important to investigate the chiral nature of $N$ and $N^*$ through $\eta$ bound states.

**Acknowledgments**

We would like to thank Prof. E. Oset for valuable discussions and carefule reading of the manuscript. The work by D.J. was supported by the Spanish Ministry of Education in the Program "Estancias de Doctores y Tecnólogos Extranjeros en España". One of us, S.H. wishes to acknowledge the hospitality of the University of Valencia where this work was done and financial support from the Foundation BBV. This work is also partly supported by the Grants-in-Aid for Scientific Research of the Japan Ministry of Education, Culture, Sports, Science and Technology (No. 14540268 and No. 11694082).

[1] C. J. Batty, E. Friedman and A. Gal, Phys. Rep. 287, 385 (1997).
[2] C. T. A. M. de Laat et al., Nucl. Phys. A523, 453 (1991).
[3] H. Toki and T. Yamazaki, Phys. Lett. B213, 129 (1988); H. Toki, S. Hirenzaki, T. Yamazaki and R. S. Hayano, Nucl. Phys. A501, 653 (1989); H. Toki, S. Hirenzaki and T. Yamazaki, Nucl. Phys. A530, 679 (1991); S. Hirenzaki, H. Toki and T. Yamazaki, Phys. Rev. C44, 2472 (1991).
[4] J. Nieves and E. Oset, Nucl. Phys. A518, 617 (1990); J. Nieves and E. Oset, Phys. Lett. B282, 24 (1992).
[5] M. Iwasaki et al., Phys. Rev. C43, 1099 (1991); R. S. Hayano, Proc. Int. Workshop on Pions in Nuclei, Penyscola, Spain (World Scientific, 1991), p. 330; A. Trudel et al., TRIUMF E628 and TRIUMF progress report (1991).
[6] N. Matsuoka et al., Phys. Lett. B359, 39 (1995).
[7] T. Yamazaki et al., Z. Phys. A355, 219 (1996); H. Gilg et al, Phys. Rev. C62, 025201 (2000).
[8] T. Waas, R. Brockmann and W. Weise, Phys. Lett. B405, 415 (1997); W. Weise, Acta Physica Polonica 31, 2715 (2000).
[9] T. Yamazaki et al., Phys. Lett. B418, 246 (1998); P. Kienle and T. Yamazaki, Phys. Lett. B514, 1 (2001).
[10] K. Itahashi et al., Phys. Rev. C62, 025202 (2000).
[11] K. Tsushima, D. H. Lu, A. W. Thomas and K. Saito, Phys. Lett. B443, 26 (1998).
[12] R.S. Hayano, S. Hirenzaki and A. Gillitzer, Eur. Phys. J. A6, 99 (1999).
[13] F. Klingl, T. Waas and W. Weise, Nucl. Phys.A650, 299 (1999).
[14] S. Hirenzaki, H. Nagahiro, T. Hatsuda and T. Kunihiro, Nucl. Phys. A. in print, `nucl-th/0208011`.
[15] R.S. Bhalerao, L.C. Liu, Phys. Rev. Lett. **54**, 865 (1985); B. Krushce *et. al.*, *ibid.* **74**, 3736 (1995); M. Benmerrouche, N.C. Mukhopadhyay *ibid.* **67**, 1070 (1991); Phys. Rev. **D51**, 3237 (1995).
[16] See reviews, T. Hatsuda and T. Kunihiro, Phys. Rep. 247, 221 (1994). G. E. Brown and M. Rho, Phys. Rep. 269, 333 (1996).
[17] C. DeTar and T. Kunihiro, Phys. Rev. **D39** (1989) 2805.
[18] D. Jido, M. Oka and A. Hosaka, Prog. Theor. Phys. **106**, 873 (2001); D. Jido, Y. Nemoto, M. Oka and A. Hosaka, Nucl. Phys. A671, 471 (2000);
[19] T. Hatsuda, M. Prakash. Phys. Lett. B **224**, (1989), 11.
[20] H. Kim, D. Jido and M. Oka, Nucl. Phys. **A640**, 77 (1998).
[21] D. Jido, N. Kodama and M. Oka, Phys. Rev. **D54**, 4532 (1996).
[22] O. Morimatsu and K. Yazaki, Nucl. Phys. A435, 727 (1985), Nucl. Phys. A483, 493 (1988).
[23] Q. Haider and L. C. Liu, Phys. Lett. B172, 257 (1986), Phys. Rev. C34, 1845 (1986).
[24] H. C. Chiang, E. Oset, and L. C. Liu, Phys. Rev. C44, 738 (1991).
[25] R. E. Chrien et al., Phys. Rev. Lett. 60, 2595 (1988).
[26] Particle Data Group, Euro. Phys. J. **51** (2000) 1.
[27] Y. Nemoto, D. Jido, M. Oka and A. Hosaka, Phys. Rev. **D57** (1998) 4124; D. Jido, T. Hatsuda and T. Kunihiro, Phys. Rev. Lett. **84**, 3252 (2000).
[28] T. Hatsuda, T. Kunihiro, and H. Shimizu, Phys. Rev. Lett. **82**, 2840 (1999); D. Jido, T. Hatsuda, T. Kunihiro, Phys. Rev. **D63**, 011901 (2000).
[29] M. Roebig-Landau *et al.*, Phys. Lett. B **373** (1996) 45.
[30] Y. K. Kwon and F. Tabakin, Phys. Rev. C18, 932 (1978).
[31] P. Berthet et al., Nucl. Phys. A443, 589 (1985).
[32] For example, I. Tanihata, J. Phys. G22, 157 (1996).
[33] T. Inoue and E. Oset, `hep-ph/0205028`; C. Garcia -Recio, J. Nieves, T. Inoue and E. Oset, `nucl-th/0206024`.